Surface & Coatings Technology 234 (2013) 114–119

Contents lists available at ScienceDirect

Surface & Coatings Technology

journal homepage: www.elsevier.com/locate/surfcoat

Atmospheric pressure microwave microplasma microorganism deactivation

D. Czylkowski [a,*], B. Hrycak [a], M. Jasiński [a], M. Dors [a], J. Mizeraczyk [a,b]

[a] Center for Plasma and Laser Engineering, The Szewalski Institute of Fluid-Flow Machinery, Polish Academy of Sciences, 14 Fiszera Str., 80-952 Gdańsk, Poland
[b] Department of Marine Electronics, Gdynia Maritime University, 83 Morska Str., 81-225 Gdynia, Poland

ARTICLE INFO

Available online 11 April 2013

Keywords:
Microwave plasma
Atmospheric pressure plasma
Microplasma
Decontamination
Sterilization

ABSTRACT

This paper is focused on the experimental investigations of microorganism decontamination by using low temperature Ar and Ar/O_2 microwave microplasma. Microplasma in the form of a microflame was generated using a simple coaxial microwave microplasma source (MmPS). The MmPS was operated at standard microwave frequency of 2.45 GHz. The electron density, microplasma temperatures and active species identification were determined on the way of Optical Emission Spectroscopy. The results of the spectroscopic measurements confirmed the MmPS usefulness in biomedical applications. The microplasma deactivation concerned two types of bacteria (*Escherichia coli*, *Bacillus subtilis*) and one fungus (*Aspergillus niger*). The investigations involved influence of the O_2 concentration, absorbed microwave power, microplasma treatment time and microplasma distance from the treated sample on the microorganism deactivation efficiency. All reported results were obtained for Ar and Ar/O_2 microplasma with gas flow rates of single l/min and O_2 admixture not exceeding 2%. The absorbed microwave power was up to 50 W. The sample treatment time was up to 10 s.

1. Introduction

Nowadays, because of many merits of an atmospheric pressure microplasma, its sources are of increasing interest from industrial point of view [1]. Microplasma is mainly characterized by a small dimension (from μm to several mm). Microplasma sources are often portable, easy to use, and cheap in production and operation. Above mentioned microplasma merits make it suitable for many applications [2–13]. Microplasma can be considered as a UV and VUV light source and can be used for gas cleaning, in microwelding, surface modification and in atomic spectroscopy systems.

Recently, there is a growing interest in the low-temperature microplasmas used in the biomedical applications such as sterilization of medical instruments, high-precision surgery, cells treatment and deactivation of bacteria and viruses [14–17]. Sterilization is a physical or chemical process that impairs or eliminates microorganisms, especially bacteria, fungus and viruses. In a plasma the sterilization is achieved due to the reactive species present in the plasma (electrons, ions, radicals, reactive molecules), UV light, etc. [18,19].

Due to many plasma sterilization systems like low pressure [20] or atmospheric pressure [21], DBD [22], RF [23], we designed, built and tested experimentally a small atmospheric pressure low-temperature microwave microplasma source (MmPS). It has structure of a coaxial line, formed by an inner conductor, made of a brass rod with a tungsten rod top, and outer conductor in the form of a brass cylinder. The MmPS is operated at standard microwave frequency of 2.45 GHz. The generated by MmPS plasma has the form of a microflame forming at the tip of the inner conductor. The main advantages of our MmPs are atmospheric pressure operation, low microplasma temperature, simplicity and low cost of manufacture. Using it we performed experimental investigations concerning microorganism deactivation by atmospheric pressure low-temperature microplasma. The investigations involved Ar and Ar/O_2 microwave microplasma treatment of two types of bacteria (*Escherichia coli*, *Bacillus subtilis*) and one fungus (*Aspergillus niger*) samples. Our motivation was to test the microplasma effect on different types of microorganisms. For that purpose we used microorganisms most commonly used as representatives of their type. *E. coli* is a Gram-negative bacteria used as the biological drinking water indicator for public health protection. Its optimal growth temperature is 37 °C. *B. subtilis* is a Gram-positive bacteria but capable of forming spores resistive to extreme environmental conditions. The optimal growth temperature range for *B. subtilis* is 25–35 °C. *A. niger* is a fungus, which can be very often found as contaminant of food, causing so called black mold on some fruits and vegetables like grapes, onions, and peanuts. The optimal temperature for its growth is 25–40 °C.

1.1. Microwave microplasma source (MmPS) and experimental setup

A number of various designs of the microplasma sources have been developed. Supply through a waveguide [24,25], consisting of coaxial line [26,27] or stripline structures [28,29] are known. Waveguide based structures, in contrast to coaxial line and stripline structures, have much bigger size and allow to operate with higher

---

[*] Corresponding author. Tel.: +48 58 69 95 244; fax: +48 58 34 16 144.
E-mail address: dczylkowski@imp.gda.pl (D. Czylkowski).

0257-8972/$ – see front matter © 2013 Elsevier B.V. All rights reserved.
http://dx.doi.org/10.1016/j.surfcoat.2013.04.010

microwave powers. The sketch and photo of our MmPS are presented in Fig. 1. It is based, as it was previously described in [30–33], on a coaxial line, formed by the inner conductor, made of a brass rod with a tungsten rod top, and outer conductor in the form of a brass cylinder. The inner conductor is fixed inside the outer conductor tightly with a PTFE centering disc. The MmPS is supplied from the microwave generator at standard frequency of 2.45 GHz through a 50 Ω coaxial line using an N-type connector. The operating gas is introduced through a duct between the inner and outer conductors. The microplasma was generated by the MmPS in the form of a tiny candle-like flame (in Ar, Ar/O_2 at low absorbed powers) or a plasma jet (in Ar/O_2 at high absorbed powers) above the inner conductor top. The length and diameter ranged from 5 to 25 mm and 0.5 to 2 mm, respectively for Ar microplasma and from 2 to 30 mm and 2 to 16 mm, respectively for Ar/O_2, depending on the operating parameters. Optionally, the MmPS could be operated with MACOR® ceramic tip. This tip played three functions: it formed a kind of nozzle that increased the velocity of gas in plasma forming zone, it prevented breakdowns between the inner and outer conductors, especially in case operating in the Ar, and it covered the hotter part of the microplasma column, thus exposing only the lowest temperature microplasma part (i.e. its tip). Fig. 2 shows photos of the microwave microplasma for various operating conditions. The operation of MmPS is described in detail in [33].

In Fig. 3 the diagram of the experimental setup used in our investigations is presented. It consists the magnetron microwave generator of frequency of 2.45 GHz equipped with circulator, microwave power measuring system (bi-directional coupler, dual-channel power meter), the MmPS, gas supplying and flow control system and spectrometer (CVI DK-480 with 1200 gr/mm and 3600 gr/mm grating) equipped with a PC computer, for emission spectra analysis. The role of the circulator is to protect the magnetron of microwave generator against damages caused by the reflected microwave power. The incident P_I and reflected P_R microwave powers were directly measured using bi-directional coupler and dual-channel power meter. There was no any impedance matching component in the experimental setup also the MmPS was not equipped with any tuning element. The photo of the experimental setup is shown in Fig. 4.

2. Results

To determine the electron density, microplasma temperatures and active species identification which could assess the usefulness of the Ar microwave microplasma for the biomedical applications, we performed spectroscopic measurements [32,33]. The measured emission spectra of the atmospheric pressure Ar microplasma in the range of 300–600 nm can be seen in Fig. 5. It was measured for Ar flow rate of 2 l/min and absorbed microwave power of 15 W. The lines identification was performed with NIST Atomic Spectra Database [34]. The H_β, OH, N_2 and NH spectral lines were observed in the emission spectrum. This is due to generation of the Ar microplasma in an ambient atmosphere. Also O atoms were detected in spectra at 615 nm [33] measured for Ar flow rate of 4 l/min and absorbed microwave power of 20 W. The electron density was determined from the Stark broadening of H_β spectral line of the hydrogen Balmer series [32] using either GKS theory of Griem, Kolb and Shen [35] or Gig-Card theory of Gigosos and Cardenoso [36]. Using SPECAIR program [37], the rotational spectra of OH radicals ($A^2\Sigma^+ \rightarrow X^2\Pi$) and N_2 molecules second positive system ($C^3\Pi \rightarrow B^3\Pi$) were employed for the determination of rotational temperatures of OH and N_2 [33]. These species were present in the microplasma due to the absorption of gases, including water vapor, from the ambient air.

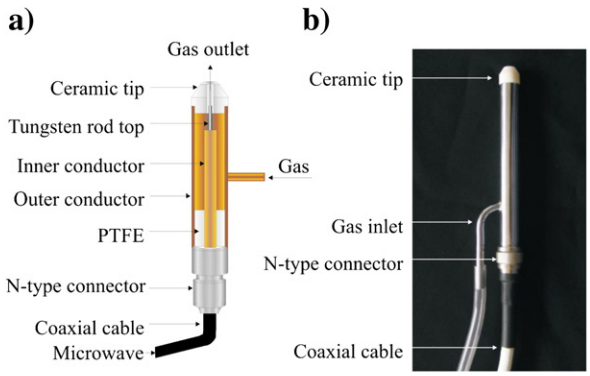

Fig. 1. Sketch (a) and photo (b) of the coaxial-line based MmPS.

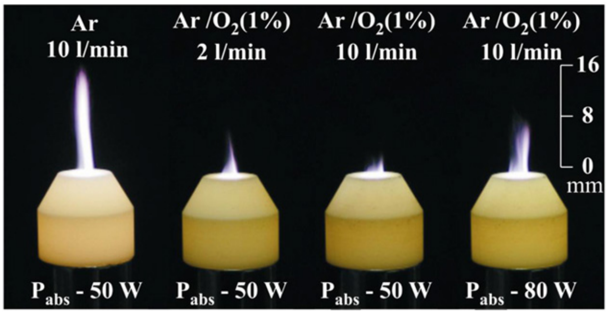

Fig. 2. Photos of the microwave microplasma for various operating conditions.

The measured electron density in Ar microplasma varied from 6×10^{14} to 1.4×10^{15} cm^{-3}, depending on operating parameters and location within the microplasma column [32,33]. When MmPS was operated with MACOR® ceramic tip, the rotational temperatures were determined to be about 500 K for OH radicals and 800 K for N_2 molecules [33]. The gas temperature at the Ar microplasma tip was as low as about 300 K [30]. This makes the microwave microplasma suitable for biomedical applications. In Fig. 6a the photo showing the possibility of human skin treatment using Ar microplasma is presented. Also the photos of the Ar microplasma treatment of the droplet of the bacteria sample on the Petri dishes and surgery scalpel are shown in Fig. 6b and c, respectively.

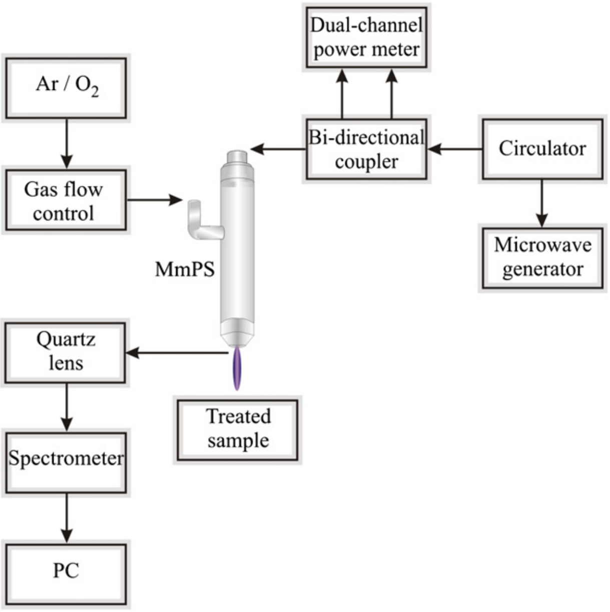

Fig. 3. Diagram of the experimental setup.